At baseline there were 12 knees with only PFJ BML (Table. Of these 12, at 48 months there was only 1 that had PF BML only, with 1 knee developing BML in the TFJ only and the other 10 developing mixed TFJ and PFJ BML.

Conclusions: The previously reported strong cross-sectional relationship between stair-climbing pain and BML volume at the PFJ at baseline, was no longer present at 48 months. Furthermore, 11 of 12 knees with only PFJ BML at baseline went on to develop BML in the TF joint. While further study is required, our results indicate that the PFJ may be important earlier in the disease process for some subjects.

Table 1
Location of BML by compartment at baseline, and at 48 months.

Baseline BML status (n=92)	BML 48mo (n=92)			
	No BML	PFJ Only	TFJ Only	Mixed
No BML (N=14)	8	0	4	2
PFJ Only (N=12)	0	1	1	10
TFJ Only (N=22)	4	0	12	6
Mixed (N=44)	1	0	7	36

Table 2
Associations of stair-climbing pain with median BML volumes – Baseline.

BML Volume	No Stair Pain (n=45)	Stair Pain (n=47)	p-value[1]
Patellofemoral	31 mm^3	388 mm^3	0.01
Patella	0 mm^3	211 mm^3	0.00
Trochlea	0 mm^3	27 mm^3	0.02
Tibiofemoral	450 mm^3	439 mm^3	0.34
Femur (weight-bearing)	0 mm^3	4 mm^3	0.24
Tibia	306 m^3	403 mm^3	0.40

[1] Wilcoxon rank sum test of the differences in medians across pain categories

Table 3
Associations of stair-climbing pain with median BML volumes – 48 months.

BML Volume	No Stair Pain (n=55)	Stair Pain (n=37)	p-value[1]
Patellofemoral	71 mm^3	164 mm^3	0.18
Patella	0 mm^3	0 mm^3	0.28
Trochlea	1 mm^3	102 mm^3	0.39
Tibiofemoral	296 mm^3	468 mm^3	0.29
Femur (weight-bearing)	19 mm^3	81 mm^3	0.06
Tibia	155 m^3	259 mm^3	0.40

[1] Wilcoxon rank sum test of the differences in medians across pain categories

382
EXTRACTION OF ANATOMICAL LANDMARKS AND AXIS FOR 3D COORDINATE SYSTEM CONSTRUCTION OF FEMUR AND TIBIA BONE MODELS

X. Cui †, H. Kim †, S. Li †, K.-S. Kwack ‡, B.-H. Min §. † *Sch. of Information and Communication Engineering, Inha Univ., Incheon, Republic of Korea;* ‡ *Dept. of Radiology, Ajou Univ. Sch. of Med., Suwon, Republic of Korea;* § *Dept. of Orthopaedic Surgery, Ajou Univ. Sch. of Med., Suwon, Republic of Korea*

Purpose: Precise positioning on the knee is crucial in to the process of observing changes in cartilage before and after arthritis surgery. A robust method for creating anatomy coordinate systems (ACS's) for three-dimensional (3-D) femur and tibia models is essential. However, it is difficult to apply traditional methods that require 3-D information from the hip and ankle joints in practical cases.

Methods: The proposed method consists of five parts as shown in Fig. 1. Firstly, a 3-D bone model is constructed from a set of binary 2-D bone images before it is smoothed. The algorithm selects the images for extracting a 3-D anatomy axis. Secondly, the centers of diaphysis regions are used to trace the centers in the 3-D model after they are calculated in the binary bone images. The principal component analysis (PCA) algorithm is applied to extract the anatomy axis from the central trace. In the 3-D model, the curvature is first calculated before the model is binarized, and then the binarized regions are labeled. Certain landmarks can be found by analyzing features of the regions. Finally, the anatomy axis and the landmarks are combined to construct a new coordinate system for the distal femur and proximal tibia as show in Fig.2. where, $\boldsymbol{P_{lm}}$ is the center point of the landmark and vector $\boldsymbol{L_a}$ represents the anatomy axis line. For constructing the ACS, firstly, determine the point $\boldsymbol{P_{lm}}$~ that is the projection of $\boldsymbol{P_{lm}}$ on $\boldsymbol{L_a}$. **O** is the origin in the new coordinate system. The vector $\boldsymbol{OP_{lm}}$ becomes the new coordinate system's x-axis. then,$\boldsymbol{OP_{lm}^{\sim}}$ is orthoginal of $\boldsymbol{L_a}$and $\boldsymbol{OP_{lm}}$.

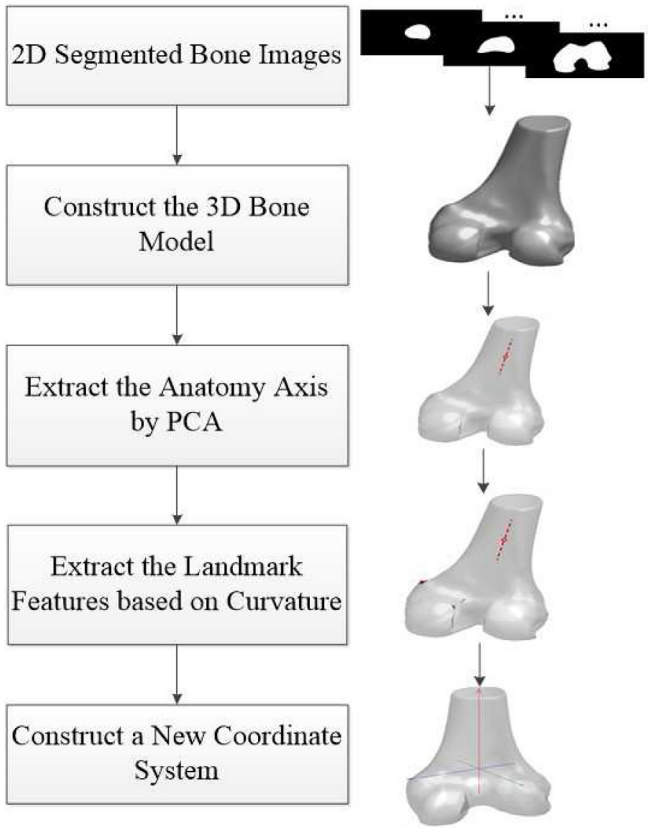

Fig.1. Flowchart of proposed new coordinate system construction.

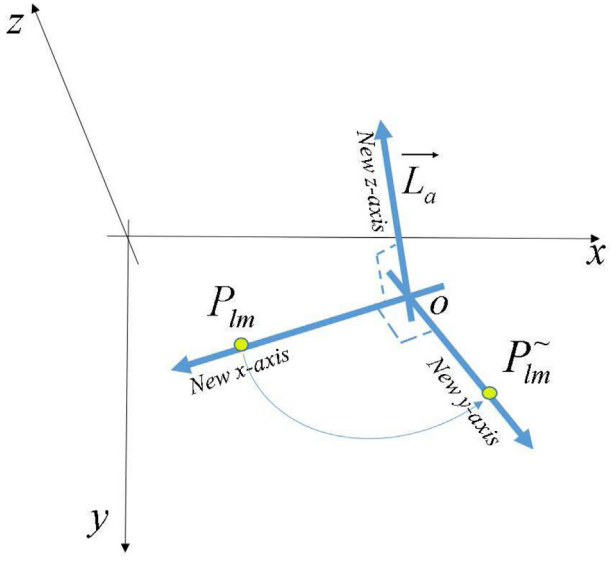

Fig.2. Construction of ACS.

Results: The proposed algorithm is applied to the distal femur and proximal tibia of knee computed tomography (CT) images from three patients. A set of manually transformed data is used to evaluate the algorithm's repeatability. The data sets were acquired from CT scans provided by Ajou University Hospital, Korea. The acquired CT images are in the DICOM image format. Information from the test data sets is shown in Table 1.

Table 1
Data Sets.

No.	Pixel spacing (*mm*)	Slice thickness (*mm*)	No. of Slice	Acquisition date
Patient_1	0.3633x0.3633	0.5	499	2010/07/26
Patient_2	0.3125x0.3125	0.5	480	2012/05/14
Patient_3	0.3379x0.3379	0.5	419	2012/05/18

The test data sets (from three different patients) were made by rotating the bone binary images by -10, -8, -5, -3, 3, 5, 8, and 10 degrees. The repeatability of the proposed method was evaluated by computing the differences in the distance and the angle for a rotated data compared to the original data. For the femur, the distance was measured between the landmark and the center of the central trace. For the tibia, the distance was measured between the landmark and the original point of the transformed coordinate.

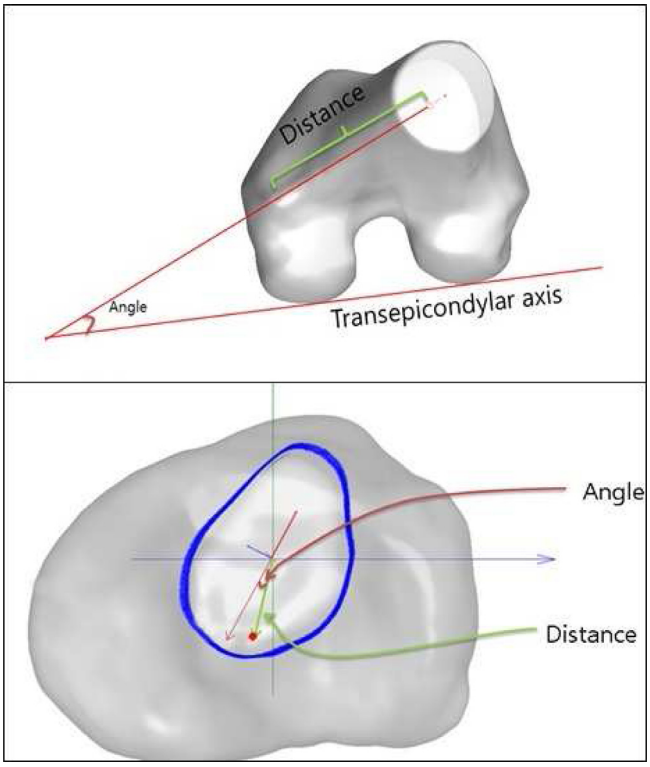

Fig.3. Distance and angle on femur and tibia.The femur angle is between the x-axis of the transformed coordinate and the transepicondylar axis of the femur. The tibia angle is between the x-axis of the transformed coordinate and the transversal diaphysis long axis. The distance and the angle of the femur and the tibia are shown in Fig. 3, where the units of the angle and the distance are degree and millimeters, respectively.Fig.4 shows the 3-D femur and tibia models in the original coordinate system (a,b) and transformed new coordinate system (c,d) acquired by the proposed method. Fig 5 shows the standard deviation of the angle and distance for both femur and tiba that computed by transformed coordinate space

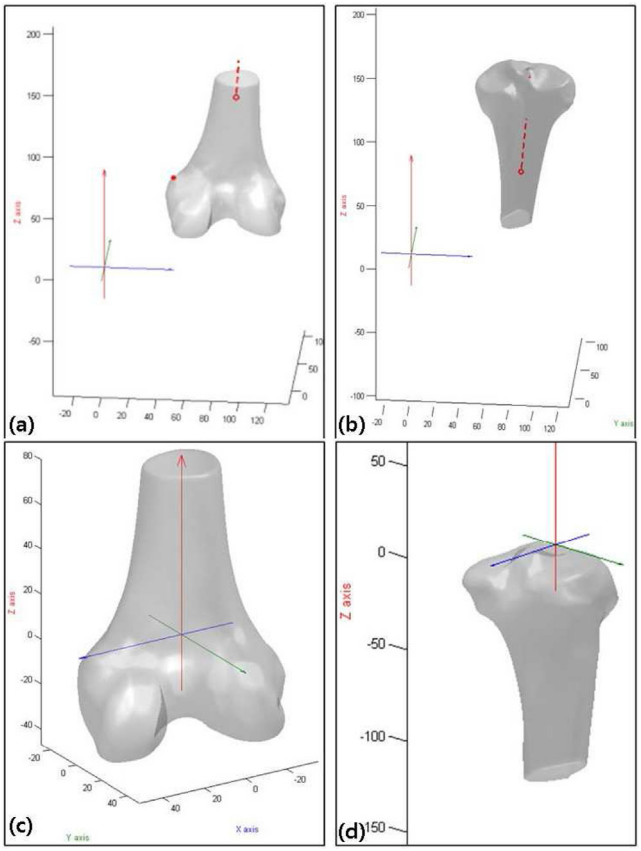

Fig.4. 3-D femur and tibia models in original and transformed coordinates.

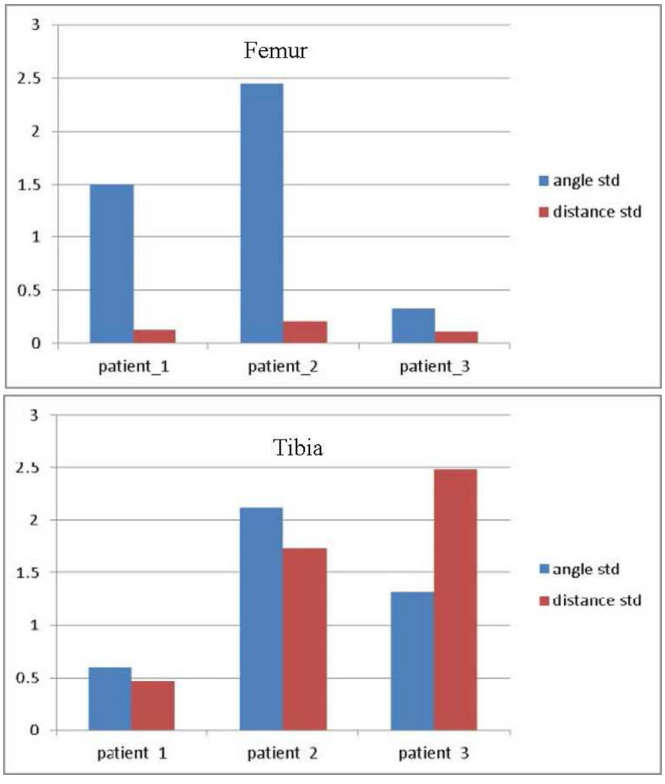

Fig.5. Standard deviations of the angle and the distance for femur and tibia.

Conclusions: This paper proposes an automated method of constructing subject-specific anatomy coordinate systems for the distal femur and proximal tibia from their 3-D bone geometries in CT images. The proposed method is able to locate the landmarks and to extract the anatomy axis automatically, and then constructs the ACS's for the femur and the tibia. Its performance is evaluated using real data sets, and the experimental results demonstrate the effectiveness and accuracy. For future works, the authors will focus on estimation of several threshold values in feature segmentation, and carry out ample tests with more CT image data sets.

383
T1RHO MAPPING OF ENTIRE FEMORAL CARTILAGE USING NOVEL DEPTH AND ANGLE DEPENDENT ANALYSIS

T. Nozaki †, Y. Kaneko †, H. Yu †, K. Kaneshiro †, R. Schwarzkopf †, T. Hara ‡, H. Yoshioka †. † *Univ. of California Irvine, Orange, CA, USA;* ‡ *Gifu Univ. Graduate Sch. of Med., Gifu, Japan*

Purpose: T1rho-weighted MR imaging has recently been proposed as an attractive biomarker to existing conventional morphological MRI methods, and has been shown to be more sensitive to biochemical change in cartilage than T2 mapping. It enables us to detect early cartilage degeneration in early osteoarthritis (OA) patients before appearing morphological change. However for the methodology of segmentation, the number of slices measured is only one or several slices, not all slices from the knee in most of reports. There is also no previous publication about normal entire femoral T1rho map profiles for analyzing regional or cartilage layer variations. These unresolved problems and limitations make diagnosis of early OA with T1rho mapping difficult clinically. The objective of this study was to create normalized T1rho profiles of healthy entire femoral cartilage with 3 dimensional (3D) angular and depth dependent analysis, and evaluate their usefulness.

Methods: 20 healthy volunteers (mean: 28.9 y.o., range: 19-38) were enrolled in this study. The study was approved by IRB, and written informed consent was obtained from each subject. Sagittal T1rho images of the knee were acquired with spoiled gradient echo (SPGR) sequence. All MR studies were performed on a 3.0-T unit (Achieva, Philips Healthcare, Netherland) utilizing an 8-channel knee receive-only RF-coil. The acquisition parameters were as follows. SPGR: mode = 3D, fat-saturation method = PROSET, TR/TE = 6.4/3.4msec, Band width = 475Hz, ETL = 64, NEX = 1, FOV = 140*140mm, Slice thickness/gap = 3/0mm, Flip angle = 10 degree, Image-matrix = 512*512mm, number of slices = 31, Time of spin-lock (TSL) = 20/40/60/80msec, acquisition time = 4min09sec *4. Entire knee cartilage segmentation was performed by two raters independently slice by slice with Matlab. T1rho depth/angle-dependent profile was investigated by partitioning cartilage into two layers (deep; 51-100% and superficial; 0-50%) and angular segmentations in step of 4-degree over the length of segmented cartilage (the angle 0 defined along B0) (Fig.1). After manual segmentation, we normalized the entire femoral cartilage with 23 new slices of all subjects. We calculated the average T1rho values of every layer in representative angles of -54,-30, 0, +34, +54 degrees to evaluate angular dependent changes including magic angle effects. We also compare T1rho values between weight bearing and non-weight bearing portion. Finally we created 3D-graph by thin-plate spline method.

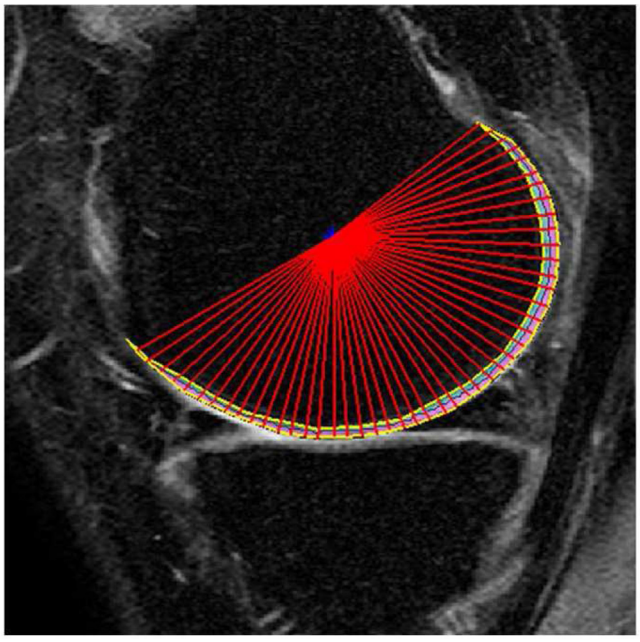

Fig.1. Sagittal SPGR images from T1rho sequence of knee MRI after manual segmentation with post-processing. Two observers segmented the entire femoral cartilage of the both images slice by slice independently. After manual segmentation, angular analysis in step of 4-degree and depth analysis with superficial and deep layers was performed automatically.

		Angle		T1rho value
Entire knee		(-180 ~ 180)	Whole	56.97 ± 2.82
			Superficial	58.94 ± 2.56
			Deep	55.68 ± 3.55
MC*	Non-weight bearing	(<-30, 30<)	Whole	57.50 ± 4.06
			Superficial	59.51 ± 4.07
			Deep	55.67 ± 5.42
	Weight-bearing	(-30 ~ 30)	Whole	54.91 ± 1.33
			Superficial	59.81 ± 1.85
			Deep	51.13 ± 2.11
LC**	Non-weight bearing	(<-30, 30<)	Whole	58.64 ± 2.47
			Superficial	60.92 ± 2.95
			Deep	56.96 ± 3.56
	Weight-bearing	(-30 ~ 30)	Whole	55.51 ± 3.34
			Superficial	62.11 ± 5.35
			Deep	52.46 ± 4.36

* MC: medial condyle **LC: lateral condyle

Fig.2. Average T1rho values in representative angles.

Results: Figure2 showed average T1rho values in representative angles. There was no influence of magic angle effect, although there was angular variation in each layer. Average T1rho values in the superficial layer of the femoral articular cartilage were higher than in the deep layer over the entire knee, medial condyle, and lateral condyle with significant difference ($p<0.05$) (Fig.3). T1rho values of the weight-bearing portion were lower than the non weight-bearing portion over the medial and lateral condyles in the deep layer with significant difference ($p<0.05$), while there was no significant difference in the superficial layer (Fig.4). The 3D-graph demonstrated cartilage T1rho values were not homogeneous over the entire knee (Fig.5).

Conclusions: T1rho values of the femoral cartilage demonstrate regional and depth variations with no significant magic angle effect. We can analyze the T1rho values across the entire femoral condyle 3 dimensionally by 3D-graphs using different displaying method from various points of view including angle, layer, slice, anatomic landmark,

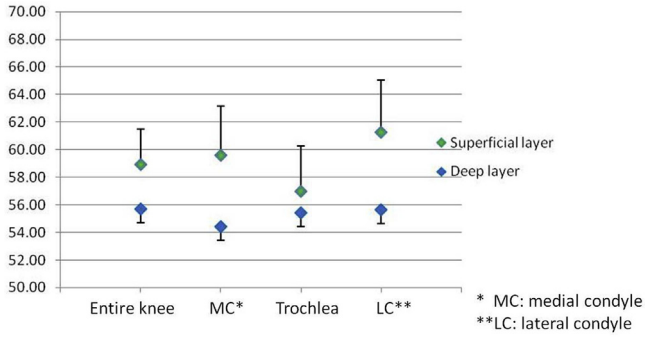

Fig.3 The difference of average T1rho values between the superficial and deep layers on each anatomical landmark. Average T1rho values in the superficial layer of femoral articular cartilage were higher than in the deep layer over the entire knee, medial condyle, and lateral condyle with significant difference ($p<0.05$)